Septin 7 forms a complex with CD2AP and nephrin and regulates glucose transporter trafficking

Anita A. Wasik[a], Zydrune Polianskyte-Prause[a], Meng-Qiu Dong[b], Andrey S. Shaw[c], John R. Yates III[b], Marilyn G. Farquhar[d], and Sanna Lehtonen[a]

[a]Department of Pathology, Haartman Institute, 00014 University of Helsinki, Finland; [b]Scripps Research Institute, La Jolla, CA 92037; [c]HHMI/Department of Pathology and Immunology, Washington University School of Medicine, St. Louis, MO 63110; [d]Department of Cellular and Molecular Medicine, University of California, San Diego, La Jolla, CA 92093

ABSTRACT **Podocytes are insulin-sensitive and take up glucose in response to insulin. This requires nephrin, which interacts with vesicle-associated membrane protein 2 (VAMP2) on GLUT4 storage vesicles (GSVs) and facilitates their fusion with the plasma membrane. In this paper, we show that the filament-forming GTPase septin 7 is expressed in podocytes and associates with CD2-associated protein (CD2AP) and nephrin, both essential for glomerular ultrafiltration. In addition, septin 7 coimmunoprecipitates with VAMP2. Subcellular fractionation of cultured podocytes revealed that septin 7 is found in both cytoplasmic and membrane fractions, and immunofluorescence microscopy showed that septin 7 is expressed in a filamentous pattern and is also found on vesicles and the plasma membrane. The filamentous localization of septin 7 depends on CD2AP and intact actin organization. A 2-deoxy-D-glucose uptake assay indicates that depletion of septin 7 by small interfering RNA or alteration of septin assembly by forchlorfenuron facilitates glucose uptake into cells and further, knockdown of septin 7 increased the interaction of VAMP2 with nephrin and syntaxin 4. The data indicate that septin 7 hinders GSV trafficking and further, the interaction of septin 7 with nephrin in glomeruli suggests that septin 7 may participate in the regulation of glucose transport in podocytes.**

Monitoring Editor
Anne Spang
University of Basel

Received: Dec 13, 2011
Revised: Jun 19, 2012
Accepted: Jul 13, 2012

INTRODUCTION

Podocytes, the visceral epithelial cells of kidney glomerulus, are terminally differentiated, highly specialized cells. They consist of the cell body and foot processes that enwrap the glomerular capillaries. Neighboring foot processes are interconnected with specialized cell adhesion structures called slit diaphragms. The slit diaphragms, together with the fenestrated endothelial cells and the glomerular basement membrane, function as a filtration barrier that prevents the passage of proteins the size of albumin and larger from the circulation into the glomerular ultrafiltrate. Upon injury, podocytes efface and detach from the basement membrane, slit diaphragms are lost, and proteinuria develops (Shankland, 2006).

Nephrin, a 180-kDa transmembrane protein of the immunoglobulin (Ig) superfamily, is the major structural component of the slit diaphragm. Mutations in the *NPHS1* gene encoding nephrin result in severe congenital nephrotic syndrome of the Finnish type (Kestila *et al.*, 1998). Nephrin associates with CD2-associated protein (CD2AP; Shih *et al.*, 2001; Palmen *et al.*, 2002), an 80-kDa cytoplasmic adapter protein that was originally found as an interaction partner of T-cell adhesion molecule CD2 (Dustin *et al.*, 1998). We identified CD2AP as a gene up-regulated during mesenchyme-to-epithelium differentiation during kidney organogenesis (Lehtonen *et al.*, 2000) and subsequently showed that CD2AP directly interacts with actin (Lehtonen *et al.*, 2002), suggesting that

This article was published online ahead of print in MBoC in Press (http://www.molbiolcell.org/cgi/doi/10.1091/mbc.E11-12-1010) on July 18, 2012.

Author contributions: A.A.W. researched data and wrote the manuscript. Z.P.-P. and M.-Q.D. researched data. A.S.S., J.R.Y., and M.G.F. reviewed/edited the manuscript. S.L. researched data and reviewed/edited the manuscript.

Address correspondence to: Sanna Lehtonen (sanna.h.lehtonen@helsinki.fi).

Abbreviations used: CD2AP, CD2-associated protein; DMSO, dimethyl sulfoxide; FCF, forchlorfenuron; FCS, fetal calf serum; GLUT1/4, glucose transporters 1/4; GST, glutathione *S*-transferase; GSV, GLUT4 storage vesicle; HIRc cells, rat fibroblasts stably expressing human insulin receptor; IFN-γ, interferon-γ; IgG, immunoglobulin G; NP-40, Nonidet P-40; PFA, paraformaldehyde; PI3K, phosphatidylinositol 3-kinase; SH3, Src homology 3; siRNA, small interfering RNA; SNAP23, synaptosome-associated protein of 23 kDa; SNARE, soluble *N*-ethylmaleimide–sensitive fusion protein attachment protein receptor; t-SNARE, target membrane SNARE; VAMP2, vesicle-associated membrane protein 2; v-SNARE, vesicle SNARE.

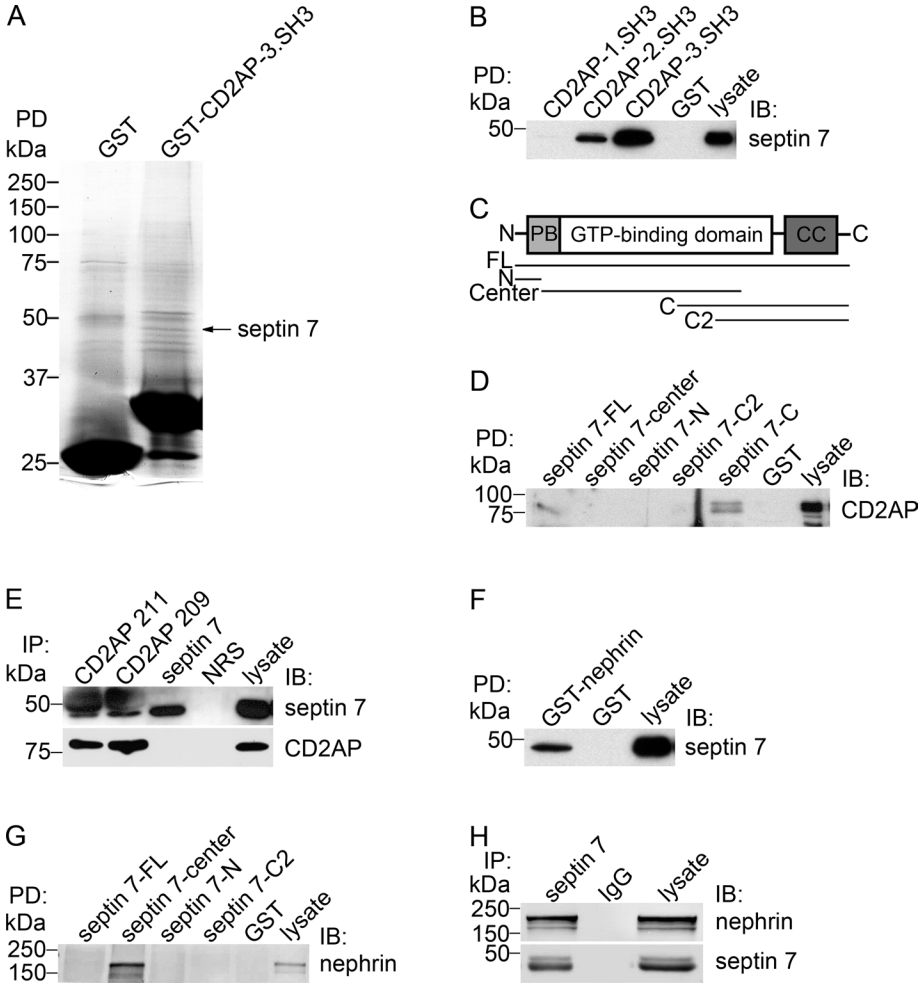

FIGURE 1: Septin 7 is a novel interaction partner of CD2AP and nephrin. (A) GST-fused 3.SH3 domain of CD2AP or GST alone were incubated with rat glomerular lysate, and the bound proteins were separated by SDS–PAGE, which was followed by staining with GelCode blue. The <50-kDa band detected in the CD2AP-GST pulldown was identified as septin 7 by mass spectrometry. (B) Septin 7 is pulled down with GST-2.SH3 and 3.SH3 domains of CD2AP, but not with GST alone, from rat glomerular lysate. (C) Schematic structure of septin 7 and GST-septin 7 fusion protein constructs used for pulldown assays. PB, polybasic region; CC, coiled-coil domain; FL, full-length (aa 1–418); N, NH_2 terminus (aa 1–31); Center, central region (aa 32–298); C, COOH terminus (aa 179–418), and C2, COOH terminus 2 (aa 244–418). (D) Pulldown assays with GST-septin 7 fusion proteins covering full-length septin 7 (septin 7-FL), septin 7-center, septin 7 NH_2 terminus (septin 7-N), and septin 7 COOH-terminal fragments (septin 7-C2 and septin 7-C) show that full-length septin 7 and the COOH terminus of septin 7 (septin-7-C) pull down CD2AP from rat glomerular lysate. (E) Two different CD2AP antibodies (CD2AP 211 and 209) coimmunoprecipitate endogenous septin 7 in HEK293 cells. Immunoprecipitation with septin 7 antibodies indicates septin 7 band immediately below the IgG heavy chain. Neither septin 7 nor CD2AP are present in immunoprecipitations with normal rabbit serum (NRS). (F) GST-nephrin cytoplasmic domain, but not GST alone, pulls down septin 7 from rat glomerular lysate. (G) Pulldown assays with GST-septin 7 fusion proteins indicate that the central domain of septin 7, but not GST alone, pulls down nephrin from rat glomerular lysate. (H) Nephrin coimmunoprecipitates with septin 7 antibodies, but not with rabbit IgG from rat glomerular lysate. Isolated glomeruli or HEK293 cells were lysed in 1% NP-40, 20 mM HEPES (pH 7.5), and 150 mM NaCl, incubated with CD2AP, septin 7, or nephrin GST-fusion proteins or antibodies, and the precipitated proteins were immunoblotted with anti-CD2AP, anti–septin 7, or anti-nephrin IgG. Glomerular or HEK293 cell lysates (10 µg) are included as control.

CD2AP may function to link membrane proteins, such as nephrin, to the actin cytoskeleton and thus stabilize the slit diaphragm (Shih *et al.*, 2001). Mice lacking CD2AP show glomerulosclerosis and foot process effacement and die of renal failure at age of 6–7 wk (Shih *et al.*, 1999). CD2AP has multiple protein–protein interaction domains, including three Src homology 3 (SH3) domains and proline-rich and coiled-coil regions, and it interacts with a number of proteins involved in various signaling and vesicular trafficking processes and thus participates in the regulation of cytoskeletal remodeling (Kirsch *et al.*, 2001; Welsch *et al.*, 2001), cytokinesis (Monzo *et al.*, 2005), apoptosis (Schiffer *et al.*, 2004), and endocytosis (Cormont *et al.*, 2003).

Diabetic nephropathy is the most common cause of progressive renal damage and occurs as a complication of reduced insulin secretion (type 1 diabetes) or sensitivity (type 2 diabetes). Interestingly, recent studies have shown that podocytes are insulin-sensitive (Coward *et al.*, 2005) and that this is essential for normal kidney function, as the podocyte-specific insulin receptor knockout mice develop significant albuminuria with histological features of diabetic nephropathy (Welsh *et al.*, 2010). This occurs in a normoglycemic environment and suggests that insulin resistance of podocytes may initiate many of the histopathological changes observed in diabetic nephropathy (Welsh *et al.*, 2010). In response to insulin, podocytes take up glucose using glucose transporters GLUT4 and GLUT1 (Coward *et al.*, 2005). This requires nephrin, which facilitates the fusion of GLUT4 and GLUT1 with the plasma membrane by interacting with vesicle-associated membrane protein 2 (VAMP2) on transport vesicles (Coward *et al.*, 2007). However, the detailed mechanisms concerning how glucose transporter trafficking, docking and fusion are regulated in podocytes and other cells remain poorly characterized. In this study we describe the identification of the small GTPase septin 7 as a novel interaction partner of CD2AP and nephrin, and show that septin 7 regulates glucose transporter trafficking.

RESULTS

Septin 7 forms a complex with CD2AP and nephrin

In pulldown assays on glomerular lysates, we found that the glutathione *S*-transferase (GST)-3.SH3 domain of CD2AP bound to a <50-kDa protein identified by mass spectrometry as septin 7 (Figure 1A). Septins are a family of cytoskeletal GTPases first discovered in the yeast as proteins required for mother–daughter separation during cytokinesis (Hartwell, 1971; Haarer and Pringle, 1987; Kim *et al.*, 1991). In mammals, septins function in cell division and in the regulation of cell polarity, cytoskeletal organization, and vesicle trafficking (Hsu *et al.*, 1998; Beites *et al.*, 1999; Kinoshita *et al.*, 2002; Kremer *et al.*, 2007). Septins are evolutionarily conserved and contain a GTP-binding domain and

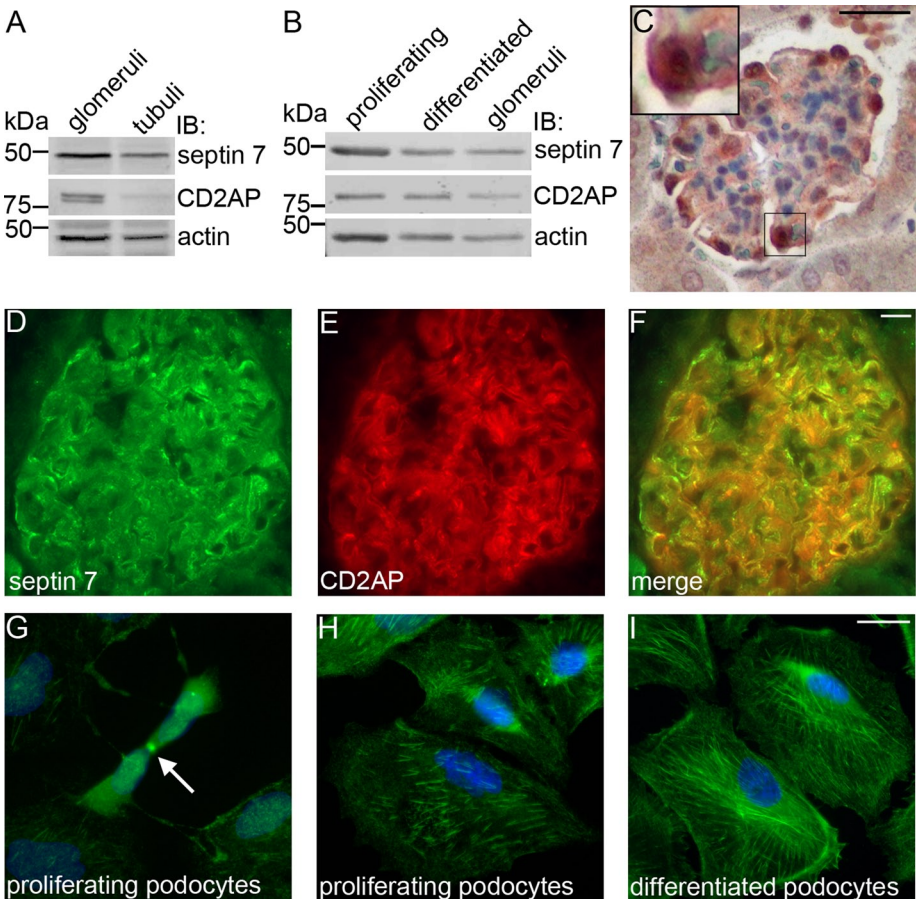

FIGURE 2: Septin 7 is expressed in podocytes. (A) Immunoblotting of rat glomerular and tubular fractions shows septin 7 expression in glomeruli and tubuli and CD2AP expression in glomeruli. (B) Septin 7 and CD2AP are expressed in both proliferating and differentiated cultured human podocytes. (C) Mouse kidney section stained with septin 7 antibody shows septin 7 expression in glomeruli, where it localizes in podocytes. Higher magnification of the boxed region is shown in the inset. Septin 7 (D) partially colocalizes with CD2AP (E) in podocytes in rat kidney sections as visualized in the merged image (F). (G) Septin 7 localizes in midbody (arrow) in proliferating podocytes and is observed in filamentous and punctate pattern in both proliferating (H) and differentiated (I) podocytes. In (A) and (B), rat glomerular and tubular fractions and cultured human podocytes were lysed in 1% NP-40, 20 mM HEPES (pH 7.5), and 150 mM NaCl, and immunoblotted with septin 7 and CD2AP IgGs and actin IgG as a loading control. (C) Adult mouse kidney paraffin sections were processed for immunoperoxidase staining, labeled with septin 7 IgG, and analyzed by light microscopy. In (D–F) and (G–I), rat kidney sections and cultured human podocytes were fixed with acetone and paraformaldehyde (PFA), respectively; labeled with septin 7 and CD2AP IgG; and examined by immunofluorescence. Scale bar: 20 μm.

variable NH_2 and COOH termini (Kinoshita, 2003; Hall *et al.*, 2005). To date, 13 septin genes have been reported in mammals, and many of them undergo alternative splicing, which means the number of septin isoforms is even greater (Kinoshita, 2003; Hall *et al.*, 2005).

To confirm that CD2AP and septin 7 form a complex and to characterize which domains of CD2AP and septin 7 mediate the interaction, we performed pulldown assays on rat glomerular lysates using CD2AP-GST fusion proteins covering each of the three SH3 domains separately and found that the 3.SH3 and 2. SH3 domains of CD2AP mediate the binding to septin 7 (Figure 1B). Pulldown assays with septin 7-GST fusion proteins covering different regions of the protein (Figure 1C) indicated that the COOH terminus of septin 7 containing the coiled-coil domain and part of the GTP-binding domain (aa 179–418) participate in the complex formation with CD2AP in rat glomeruli (Figure 1D).

To further confirm the physiological interaction of CD2AP and septin 7, we performed coimmunoprecipitation assays of endogenous proteins in HEK293 cells with two different CD2AP antibodies. Immunoblotting of the precipitates with septin 7 antibodies confirmed that CD2AP and septin 7 form a complex (Figure 1E). Collectively CD2AP and septin 7 are found in the same complex, and the SH3 domains of CD2AP and the COOH terminus of septin 7 mediate the formation of the complex.

Because CD2AP forms a complex with nephrin, we analyzed whether septin 7 is also part of the nephrin protein complex. Pulldown assay on rat glomerular lysate indicated that GST-nephrin cytoplasmic domain pulls down septin 7 (Figure 1F) and further, that the central region (aa 32–298) of septin 7 pulls down nephrin (Figure 1G). Immunoprecipitation of rat glomerular lysate with septin 7 antibodies, followed by detection with nephrin antibodies, indicated that septin 7 coimmunoprecipitates with nephrin in rat glomeruli (Figure 1H).

Septin 7 partially colocalizes with CD2AP in human podocytes

Septin 7 is widely expressed in human tissues (Hall *et al.*, 2005) but has not been previously studied in the kidney. To confirm the expression of septin 7 in glomeruli, we immunoblotted isolated rat glomerular and tubular fractions and found that septin 7 is expressed in both glomeruli and tubules, and CD2AP is concentrated in glomeruli (Figure 2A). We also used immunoblotting to study the expression of both proteins in cultured human podocytes and found septin 7 and CD2AP in both proliferating and differentiated podocytes (Figure 2B). Immunoperoxidase staining of mouse kidney sections confirmed that septin 7 localizes in podocytes in vivo (Figure 2C) and further, double immunolabeling of kidney sections with septin 7 and CD2AP antibodies revealed partial colocalization of the proteins (Figure 2, D–F) further suggesting their interaction. In proliferating podocytes, septin 7 localized in the midbodies of cells undergoing cytokinesis (Figure 2G), and in both proliferating and differentiated podocytes, it appeared as filaments and in a punctate pattern in the cytoplasm (Figure 2, H–I).

Localization of septin 7 in podocytes depends on an intact actin cytoskeleton and CD2AP

As mammalian septins have been reported to localize along actin filaments (Kinoshita *et al.*, 1997), and we found septin 7 to localize in a filamentous pattern in human podocytes, we double labeled podocytes with septin 7 antibodies and phalloidin to visualize filamentous actin. In proliferating and differentiated podocytes, septin 7 is expressed as short filaments that partially align along actin stress

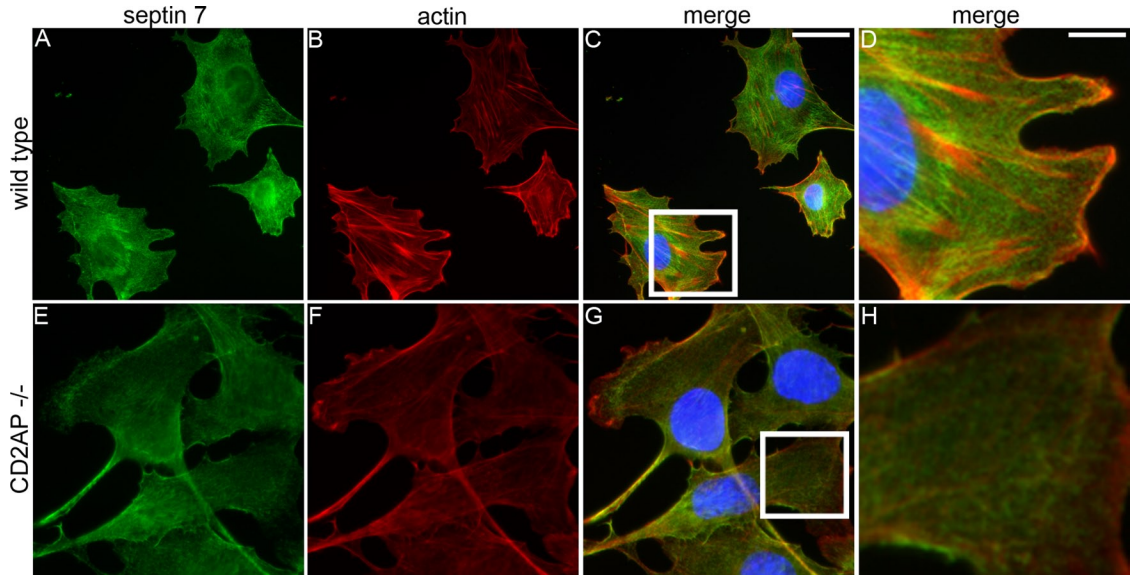

FIGURE 3: Localization of septin 7 depends on CD2AP. Double labeling of wild-type (A–D) and CD2AP$^{-/-}$ (E–H) mouse podocytes for septin 7 (green) and actin (red). Nuclei are visualized with Hoechst (blue). (A–D) In wild-type podocytes, septin 7 filaments (A) partially align along actin stress fibers detected with phalloidin (B–D). (E–H) In CD2AP$^{-/-}$ podocytes, septin 7 filaments disappear. Boxed regions indicated in (C and G) are magnified in (D and H), respectively. Cultured mouse podocytes were fixed with PFA, labeled with septin 7 IgG and phalloidin, and examined by fluorescence microscopy. Scale bars: 20 μm (A–C and E–G); 7 μm (D and H).

fibers (Supplemental Figure S1, A–D and I–L). In several cell types, the localization of septins depends on an intact actin cytoskeleton (Kinoshita *et al.*, 1997; Schmidt and Nichols, 2004). To analyze whether this is also the case in podocytes, we used cytochalasin D to disrupt filamentous actin organization. This changed septin 7 organization in podocytes: a fraction of normally linear septin 7 filaments curled and localized in rings (Figure S1, E–H and M–P). The filamentous distribution of septin 7 thus depends on an intact actin cytoskeleton in human podocytes. The localization of CD2AP also depends on an intact actin cytoskeleton; in podocytes treated with cytochalasin D, CD2AP appears as aggregates largely colocalizing with the collapsed actin (Figure S2).

To analyze whether the localization of septin 7 depends on CD2AP, we stained CD2AP$^{-/-}$ mouse podocytes and wild-type podocytes with septin 7 antibodies and phalloidin. In wild-type podocytes, septin 7 is expressed as short filaments that partially align along actin stress fibers (Figure 3, A–D), whereas in CD2AP$^{-/-}$ podocytes, loss of CD2AP is associated with the disappearance of actin stress fibers and septin 7 filaments (Figure 3, E–H).

Septin 7 interacts with septin 9 and septin 11 in human podocytes

Mammalian septins form homo-oligomers in vitro and hetero-oligomeric polymers in vitro and in vivo (Joberty *et al.*, 2001; Nagata *et al.*, 2004). Previous studies demonstrate that septin 7, septin 9, and septin 11 are components of in vivo septin complexes isolated from REF52 cells (Nagata *et al.*, 2004). Several isoforms of septin 9 seen as multiple bands by SDS–PAGE are expressed in cultured podocytes (Figure S3A). Septin 11 antibody recognized a 49-kDa band in podocytes (Figure S3B). The possible interaction of septin 7 with septins 9 and 11 was analyzed by immunoprecipitation assay and showed that septin 7 forms a complex with septin 9 and septin 11 in differentiated podocytes (Figure S3C).

Because loss of one septin destabilizes the others (Kinoshita *et al.*, 2002), we depleted septin 7 by small interfering RNA (siRNA) in human podocytes and examined the expression of septin 9 and septin 11 (Figure S3D). In septin 7–depleted podocytes, septin 7 expression was reduced by 60.5% (58–62.4%), septin 9 by 64.5% (54.1–67.5%), and septin 11 by 61% (60–62%), compared with the control siRNA-transfected podocytes (Figure S3E). This suggests that knockdown of septin 7 destabilizes the other members of the septin 7 protein complex in human podocytes.

Septin 7 knockdown or alteration of septin assembly increases glucose uptake in HIRc cells and podocytes

Mammalian septins have several functions in addition to their role in cytokinesis. They are also present in nondividing neurons, in which they regulate exocytosis (Hsu *et al.*, 1998; Beites *et al.*, 1999). As we found that septin 7 coimmunoprecipitates with nephrin, and nephrin is known to be involved in GLUT4 storage vesicle (GSV) fusion with the plasma membrane, we speculated that septin 7 could also affect GSV trafficking and thus regulate glucose uptake. To analyze this, we used HIRc cells, rat fibroblasts stably expressing human insulin receptor. Introduction of a pool of four septin 7 siRNAs into HIRc cells resulted in an 81% (65.4–92%) decrease in the abundance of septin 7 compared with control siRNA-transfected cells (Figure 4A). Also septin 9 and septin 11 levels were reduced by 55 and 21%, respectively, in septin 7 siRNA-treated cells (unpublished data), indicating that knockdown of septin 7 in HIRc cells also destabilizes other septins in the complex.

We next measured the uptake of 2-deoxy-D-glucose into HIRc cells transfected with septin 7 siRNA and found a 19% increase compared with control siRNA-transfected cells in basal state (Figure 4B). In serum-starved cells, knockdown of septin 7 increased the glucose uptake by 17% (Figure 4C). After insulin stimulation, the activity increased by 144% (64.6–179.8%) in the septin 7 knockdown cells, whereas the increase in control siRNA-transfected cells was 90% (32.1–144.1%) (Figure 4C). Glucose uptake activity of the control siRNA-transfected and serum-starved cells was set to 100% (Figure 4C).

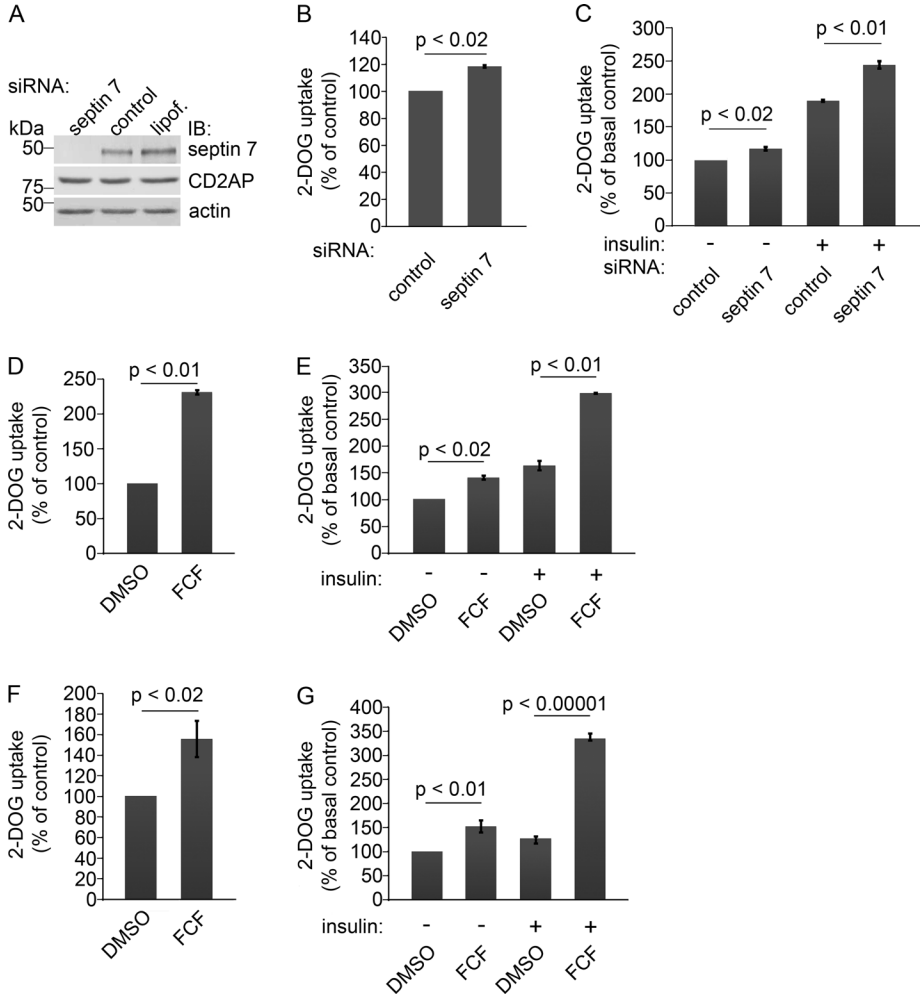

FIGURE 4: Knockdown of septin 7 or alteration of the assembly of septins increases glucose uptake in HIRc cells and podocytes. (A) Septin 7 siRNA leads to 81% reduction in septin 7 expression in HIRc cells. CD2AP expression level remains unchanged in septin 7 knockdown cells. HIRc cells were transfected with rat septin 7 SMARTpool siRNA (septin 7), siCONTROL Non-Targeting Pool siRNA (control), or Lipofectamine 2000 alone (lipof.), and analyzed by immunoblotting 72 h after transfection. Actin is included as a loading control. (B) Depletion of septin 7 increases the glucose uptake activity of HIRc cells by 19% compared with the control siRNA-transfected cells (set to 100%) in basal state. (C) Knockdown of septin 7 increases the glucose uptake activity of HIRc cells by 17% in serum-starved cells (septin 7 siRNA, – insulin) and by 144% after insulin stimulation (septin 7 siRNA, + insulin). The increase in glucose uptake in control siRNA-transfected cells is 90% after insulin stimulation (control siRNA, + insulin). Glucose uptake activity of the control siRNA-transfected and serum-starved cells is set to 100% (control siRNA, – insulin). (D) HIRc cells treated with FCF show 131% increase in glucose uptake activity in basal state compared with solvent only–treated cells (DMSO, set to 100%). (E) FCF treatment increases the glucose uptake activity of HIRc cells by 41% in serum-starved cells (FCF, – insulin) and by 198% after insulin stimulation (FCF, + insulin). The increase in glucose uptake in solvent only–treated cells is 64% after insulin stimulation (DMSO, + insulin). Glucose uptake activity of the solvent only–treated and serum-starved cells is set to 100% (DMSO, – insulin). (F) Alteration of septin assembly by FCF in mouse podocytes leads to a 56% increase in glucose uptake in basal state. (G) FCF treatment increases the glucose uptake activity of mouse podocytes by 52% in serum-starved cells (FCF, – insulin) and by 235% after insulin stimulation (FCF, + insulin). Solvent only–treated mouse podocytes show a 27% increase in glucose uptake after insulin stimulation (DMSO, + insulin). HIRC cells were transfected with septin-7 siRNA (A–C) or treated with 50 μM FCF (D and E), and glucose uptake was measured as described in *Materials and Methods* in basal state (B and D) or after serum starvation (–) and treatment with 200 nM insulin (+) (C and E). Mouse podocytes were treated with 50 μM FCF for 4 h (F and G) and treated (+) or not (–) with 20 nM insulin (G). Bars show the mean and error bars show the SD of three independent experiments using Student's *t* test.

To confirm the results, we used two individual septin 7 siRNAs and found that they reduced the level of septin 7 by 72 and 60% (Figure S4, A and B). They also reduced the level of septin 9 and septin 11 (Figure S4, A and B), and increased glucose uptake by 57% (56.3–58.1%) and 37% (34.1–41.7%) under basal conditions (Figure S4, C and D), further confirming the specificity of the septin 7 knockdown. The data indicate that septin 7 functions as a negative regulator of glucose uptake in HIRc cells.

To further confirm that septin 7 regulates glucose uptake, we used forchlorfenuron (FCF), previously shown to disrupt septin localization in budding yeast (Iwase *et al.*, 2004) and to alter the assembly and dynamics of septins, but not of actin or microfilaments, in mammalian cells or in polymerization assays in vitro (Hu *et al.*, 2008). Importantly, FCF treatment causes similar functional effects as septin depletion by siRNA (Hu *et al.*, 2008). HIRc cells treated with FCF, which was followed by 2-deoxy-D-glucose uptake assay, showed a 131% (76.6–170%) increase in glucose uptake in basal state compared with solvent only–treated cells (Figure 4D). After serum starvation, FCF treatment increased the glucose uptake by 41% (36.2–45.8%; Figure 4E). Insulin stimulation increased the glucose uptake activity by 198% (196–201%) in the FCF-treated cells, whereas the increase in insulin-stimulated, solvent only–treated cells was 64% (57.3–70.6%; Figure 4E). Glucose uptake activity of the serum-starved and solvent only–treated cells was set to 100% (Figure 4E).

To analyze whether septins also regulate glucose uptake in podocytes, we treated mouse podocytes with FCF. A 2-deoxy-D-glucose uptake assay showed a 56% (33.6–64.1%) increase in glucose uptake in FCF-treated podocytes in basal state compared with podocytes treated with solvent only (Figure 4F). In serum-starved podocytes, FCF treatment increased the glucose uptake by 52% (45.6–62%; Figure 4G), and serum starvation followed by insulin stimulation led to a 235% (190–264%) increase in glucose uptake in FCF-treated podocytes, whereas the increase in insulin-stimulated, solvent only–treated podocytes was 27% (21.4–31%; Figure 4G). This indicates that septins play an important role in the regulation of glucose uptake in podocytes. We also examined whether FCF has an effect on septin organization in podocytes. FCF treatment changed septin 7 organization to bundle-like filaments that accumulated at the cell periphery. FCF did not affect actin cytoskeleton organization (Figure S5).

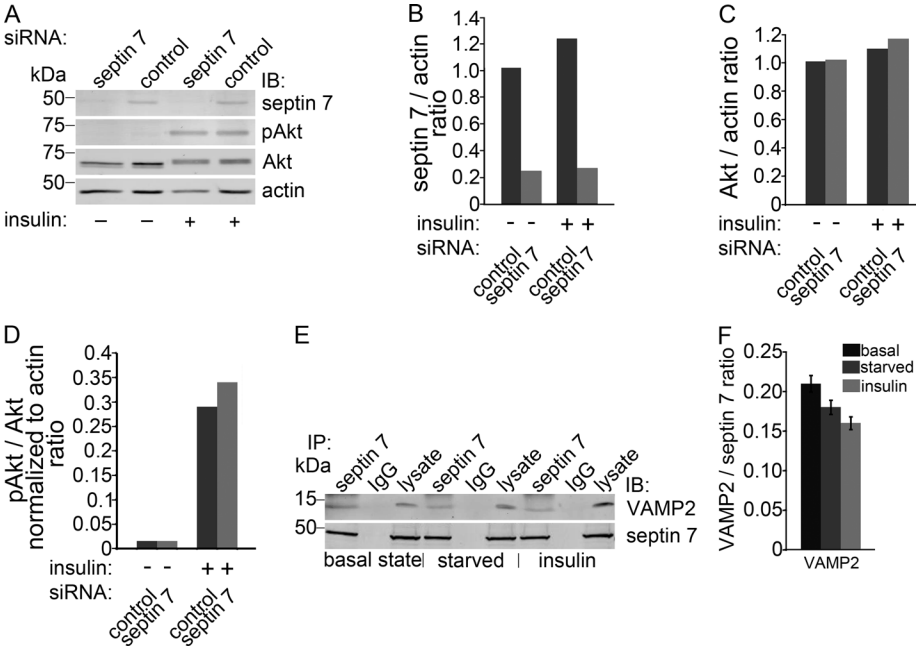

FIGURE 5: Septin 7 forms a complex with VAMP2 involved in vesicle trafficking. (A) Knockdown of septin 7 does not affect the activity of insulin-mediated Akt signaling pathway. HIRc cells transfected with septin 7 or control siRNA were serum-starved and untreated (–) or treated (+) with 200 nM insulin and immunoblotted with septin 7, pan-Akt (Akt), phospho-Akt (pAkt), and actin IgG. Akt phosphorylation is unaffected by septin 7 depletion. Representative blot of three independent experiments. (B) Quantification of septin 7 level in (A) presented as septin 7:actin ratio. (C) Quantification of total Akt level in (A) presented as Akt:actin ratio. (D) Quantification of pAkt levels in (A) presented as pAkt:total Akt normalized to actin ratio. (E) VAMP2 coimmunoprecipitates with septin 7 but not with control IgG in HIRc cells in basal state and in serum-starved and insulin-stimulated cells. Lysate, 10 μg. (F) Quantification of protein levels of three replicate blots as in (E) presented as VAMP2:septin 7 ratio showing that insulin stimulation does not affect the interactions as the difference in complex formation between different conditions did not reach statistical significance.

Knockdown of septin-7 does not affect the activity of the phosphatidylinositol 3-kinase (PI3K) pathway

To elucidate the mechanism of septin 7 knockdown negatively regulating glucose uptake, we examined the phosphorylation of Akt, which indicates the activation of the phosphatidylinositol 3-kinase (PI3K) pathway, in insulin-stimulated HIRc cells treated with septin 7 siRNA. Depletion of septin 7 had no effect on the total level of Akt or on the insulin-stimulated phosphorylation of Akt (Figure 5, A–D), indicating that loss of septin 7 does not affect insulin signal transduction.

Septin 7 interacts with VAMP2 involved in vesicle trafficking

GSV trafficking consists of several steps, including targeting of the vesicles to the site of fusion followed by soluble *N*-ethylmaleimide–sensitive fusion protein attachment protein receptor (SNARE) complex formation between the v-SNARE VAMP2 and the t-SNAREs syntaxin 4 and synaptosome-associated protein of 23 kDa (SNAP23; Rothman, 1994; Weber *et al.*, 1998). To analyze whether septin 7 could be involved in GSV trafficking, we performed coimmunoprecipitations on HIRc cell lysates with septin 7 antibody and found that septin 7 coimmunoprecipitates VAMP2 (Figure 5E) and that the interaction does not depend on insulin stimulation (Figure 5, E and F). This suggests that septin 7 could be involved in regulating GSV trafficking.

Septin 7 is found in cytosolic and membrane fractions

Interaction of septin 7 with the vesicle protein VAMP2 and plasma membrane protein nephrin prompted us to study the localization of septin 7 in subcellular fractions. In mouse podocytes, septin 7 is present in both the membranes and cytosol (Figure S6A), and insulin stimulation does not change the partitioning of septin 7 in the fractions (Figure S6, B and C). The effectiveness of insulin stimulation was confirmed by immunofluorescence staining showing partial translocation of GLUT4 to the plasma membrane after insulin stimulation (Figure S6, D–F). To define the intracellular localization of septin 7 more precisely and to see whether it changes upon insulin stimulation, we studied septin 7 localization by confocal microscopy in cultured mouse podocytes using flotillin2 as the membrane marker. Septin 7 was found in a filamentous and vesicular pattern in the cytoplasm and on the plasma membrane in mouse podocytes at basal state, and its localization did not significantly change after serum starvation or insulin stimulation (Figure S7, A, E, and I). Septin 7 partially colocalized with flotillin2 on the plasma membrane in basal state and in serum-starved and insulin-stimulated cells (Figure S7).

Septin 7 depletion facilitates GSV fusion with the plasma membrane

As nephrin facilitates GSV fusion with the plasma membrane by interacting with VAMP2 (Coward *et al.*, 2007), we went on to investigate the effect of septin 7 knockdown on the complex formation between nephrin and VAMP2. HIRc cells were transfected with septin 7 siRNA; this was followed by overexpression of nephrin by viral infection (Figure 6A). Septin 7 knockdown increased the association between nephrin and VAMP2 and also between syntaxin 4 and VAMP2 (Figure 6, B–D). This, together with the finding that septin 7 forms a complex with both nephrin and GSV component VAMP2, indicates that septin 7 may form a filamentous barrier and thus hinder vesicle trafficking, and consequently, depletion of septin 7 facilitates the fusion of the vesicles with the plasma membrane.

DISCUSSION

Septins form hetero-oligomeric complexes (Hsu *et al.*, 1998; Kinoshita *et al.*, 2002), and we found a complex of three septins—septin 7, septin 9 and septin 11—in cultured human podocytes. A similar septin complex was previously identified in rat embryonic fibroblasts (Nagata *et al.*, 2004). Knockdown of one septin often leads to reduced levels of the other septins in the complex (Kinoshita *et al.*, 2002), and we found this to be true in both podocytes and HIRc cells. The distribution of septins in HeLa cells and NIH 3T3 fibroblasts depends on an intact actin cytoskeleton (Kinoshita *et al.*, 1997; Kinoshita *et al.*, 2002), and our data indicate that the filamentous organization of septin 7 in podocytes also depends on intact actin architecture.

The partial overlap of septin 7 filaments with actin stress fibers in podocytes suggests that septin 7 association with actin is mediated by other molecules. Anillin has been suggested to mediate the association of septins with actin during cytokinesis (Kinoshita *et al.*, 2002), but anillin is mostly sequestered in the nucleus during

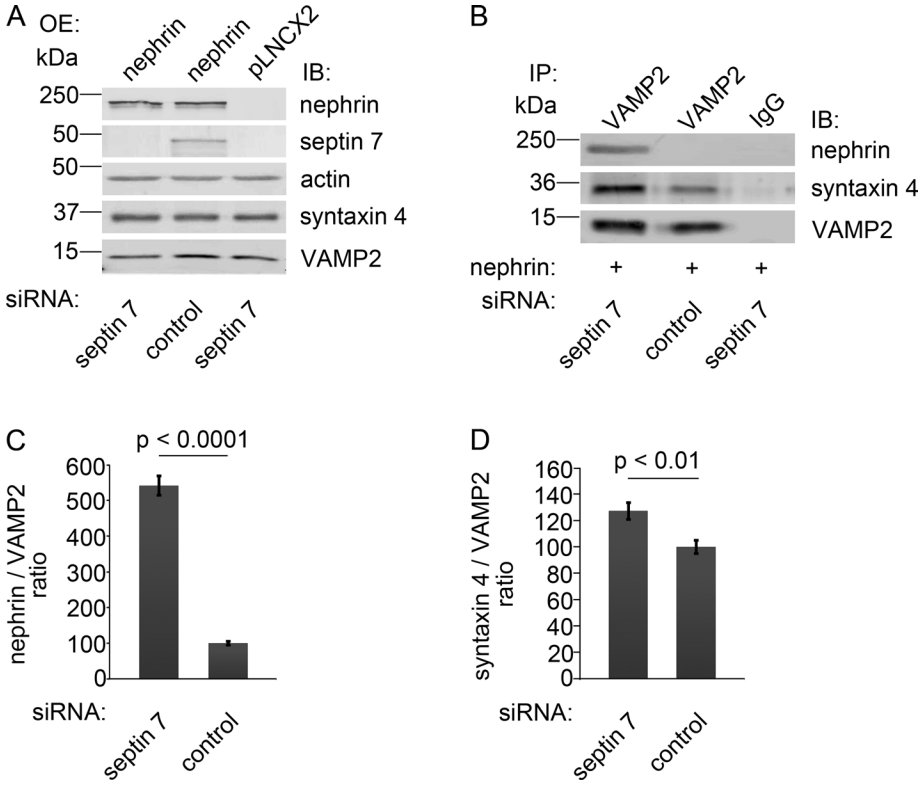

FIGURE 6: Knockdown of septin 7 increases complex formation between nephrin and VAMP2, and between syntaxin 4 and VAMP2. (A) HIRc cells were transfected with septin 7 or control siRNA, which was followed by nephrin or empty vector (pLNCX2) overexpression (OE) by viral infection. Immunoblotting confirms nephrin overexpression and septin 7 depletion. Syntaxin 4 and VAMP2 levels remain constant. (B) Cell lysates of HIRc cells, transfected with septin 7 or control siRNA and overexpressing nephrin, were immunoprecipitated with anti-VAMP2 antibodies and immunoblotted with nephrin, syntaxin 4, and VAMP2 antibodies. Depletion of septin 7 increases the interaction of VAMP2 with nephrin and syntaxin 4. (C and D) Quantification of protein levels of three replicate blots as in (B). The bars represent nephrin:VAMP2 (C) and syntaxin 4:VAMP2 (D) ratios. Bars show the mean and error bars show the SD using Student's *t* test.

interphase (Oegema *et al.*, 2000). The fact that CD2AP binds actin directly (Lehtonen *et al.*, 2002), localization of CD2AP depends on an intact actin architecture (Lehtonen *et al.*, 2002, and this study), and CD2AP and septin 7 interact suggest that CD2AP may mediate binding of septin 7 to actin during interphase. Further, we found that septin 7 localization depends on CD2AP; in CD2AP$^{-/-}$ podocytes that show loss of actin stress fibers (Yaddanapudi *et al.*, 2011), septin 7 loses its filamentous expression pattern. We did not determine whether septin 7 binds CD2AP directly, but we found that the SH3 domains of CD2AP and the COOH terminus of septin 7 (aa 179–418) containing the coiled-coil domain and part of the GTP-binding domain participate in the formation of the complex. This, together with the lack of the proline-rich domain (that binds SH3 domains) in septin 7 and its presence in septin 9 (Hall and Russell, 2004), suggests that the interaction could be mediated by septin 9. Also, part of the GTP-binding domain of septin 7 is important for the interaction, as a shorter construct (aa 244–418) did not bind CD2AP.

We found that septin 7 concentrates in the midbody in proliferating podocytes, suggesting it can also participate in regulating cell division in podocytes. However, mature podocytes in vivo are terminally differentiated and do not divide. In postmitotic neurons, septins regulate exocytosis (Hsu *et al.*, 1998; Beites *et al.*, 1999; Vega and Hsu, 2003). We found that septin 7 also regulates exocytosis and, specifically, we show that septin 7 inhibits GSV trafficking and glucose uptake. Glucose uptake in septin 7–depleted cells and in cells treated with FCF, affecting all septins, increased under basal conditions, but the increase was more pronounced after insulin stimulation, suggesting that septins may affect constitutional glucose transporter GLUT1 in addition to regulating insulin-stimulated glucose transporter GLUT4.

To define the mechanism of septin 7 regulation of glucose uptake, we first examined whether septin 7 ablation affects the insulin-stimulated activation of the PI3K signaling pathway, but found no effect suggesting that septin 7 regulates GSV trafficking. On targeting of vesicles to the plasma membrane, a complex of SNARE proteins, consisting of syntaxin and SNAP on the target membrane (t-SNAREs) and VAMP2 on the vesicle (v-SNARE), form a complex to promote the fusion (Söllner *et al.*, 1993). We found that septin 7 interacts with VAMP2 and nephrin, which are regulators of vesicle trafficking on GSVs and the plasma membrane (Coward *et al.*, 2007), respectively, and we showed by subcellular fractionation that septin 7 is found in both cytosolic and membrane fractions in basal state, serum-starved, and insulin-stimulated mouse podocytes. Previously, two models were proposed to explain how septin-5/CDCrel-1, predominantly found in the brain in postmitotic neurons (Beites *et al.*, 1999), could tether vesicles away from the plasma membrane. Septins could either physically restrict the movement of the vesicles to the plasma membrane by binding to v-SNAREs and t-SNAREs, or they could create a grid-like physical barrier along the plasma membrane, thus preventing fusion of the vesicles (Beites *et al.*, 2005). Our data on podocytes and HIRc cells suggest that septin 7 could function by hindering the movement of the GSVs. The interaction of septin 7 with nephrin in glomeruli suggests that they may function together in regulating GSV trafficking in glomeruli in vivo.

Podocytes are known to be targets for insulin (Coward *et al.*, 2005) and can develop insulin resistance as podocytes isolated from db/db mice lose the ability to respond to insulin (Tejada *et al.*, 2008). Further, the deletion of insulin receptor specifically in podocytes leads to the development of albuminuria and histological features recapitulating diabetic nephropathy (Welsh *et al.*, 2010). The data suggest that insulin resistance of podocytes may be a causative factor initiating the development of certain pathological processes observed in diabetic nephropathy (Welsh *et al.*, 2010). The molecular targets of insulin resistance may, in addition to the insulin receptor itself, involve its downstream signaling events or the regulatory proteins participating in glucose transporter trafficking, docking, and fusion events. Nephrin regulates glucose uptake in podocytes by interacting with VAMP2 and facilitates the fusion of the GSVs with the plasma membrane, apparently functioning as a modifying protein in the SNARE complex (Coward *et al.*, 2007). Otherwise, the mechanisms regulating glucose transporter trafficking and glucose

uptake in podocytes are uncharacterized. In this study, we found that septin 7 interacts with both nephrin and SNARE complex proteins and negatively regulates glucose uptake, as knockdown of septin 7 strengthened the interaction between nephrin and VAMP2, and also between syntaxin 4 and VAMP2. This, together with the previous models proposed for septin-5/CDCrel-1 (Beites *et al.*, 2005), further supports the idea that septin 7 also may form a physical barrier that hinders GSV trafficking.

Collectively our data show that septin 7 negatively regulates glucose uptake in both HIRc cells and podocytes. Septin 7 may hinder GSV trafficking by forming a physical barrier between the vesicles and the plasma membrane by associating with v-SNAREs and nephrin. Further, interaction of septin 7 with nephrin in glomeruli in vivo suggests a role for septin 7 in regulating vesicle trafficking in podocytes. These results suggest that the regulators of glucose transporter trafficking may provide suitable targets to enhance insulin sensitivity of podocytes and thus to prevent the development and progression of diabetic nephropathy.

MATERIALS AND METHODS

Preparation of tissue lysates

Glomerular and tubular fractions were isolated from kidney cortices of male Sprague Dawley rats by graded sieving (Orlando *et al.*, 2001) and lysed in Nonidet P-40 (NP-40) lysis buffer (1% NP-40, 20 mM HEPES, pH 7.5, 150 mM NaCl) supplemented with 50 mM NaF, 1 mM Na_3VO_4 and 1× Complete Proteinase Inhibitor Cocktail (Roche, Basel, Switzerland) at 4°C for 30 min. Detergent-insoluble material was removed by centrifugation (16 000 × *g* at 4°C for 15 min).

Cell culture and preparation of cell lysates

Conditionally immortalized human podocytes (AB 8/13) were maintained in RPMI-1640 supplemented with 10% fetal calf serum (FCS) and 1% ITS (Sigma-Aldrich, St. Louis, MO) at 33°C and were shifted to 37°C for 2 wk for differentiation (Saleem *et al.*, 2002). Mouse wild-type and CD2AP$^{-/-}$ podocytes and HEK293 and HEK293FT cells were maintained in DMEM containing 4.5 g/l glucose, 10% FCS, penicillin, and streptomycin (Sigma-Aldrich), supplemented with 10 U/ml IFN-γ (Sigma-Aldrich) for podocytes. Rat-1 fibroblasts overexpressing wild-type human insulin receptor (HIRc cells) were maintained in DMEM containing 1g/l glucose, 10% FCS, penicillin, and streptomycin at 37°C. Cell lysates were prepared as above in NP-40 lysis buffer or in 0.5% NP-40, 100 nM NaCl, 20 nM Tris-HCl, pH 8.0, and 1 mM EDTA for immunoprecipitation of VAMP2.

Pulldown assays, mass spectrometry, and immunoblotting

GST, GST-CD2AP SH3 domains (Palmen *et al.*, 2002), GST-nephrin (Lehtonen *et al.*, 2004), and GST-septin 7 (Nagata *et al.*, 2004) fusion proteins encompassing the full-length protein (aa 1–418), the NH_2 terminus (aa 1–31), the central region (aa 32–298), the COOH terminus (aa 179-418), or the COOH terminus 2 (aa 244–418) were expressed in BL21(DE3) (Stratagene, La Jolla, CA) and purified on glutathione-Sepharose beads (Invitrogen, Camarillo, CA). Pulldown assay was performed as in Lehtonen *et al.* (2004). For mass spectrometry analysis, the precipitated proteins were separated in SDS–PAGE and stained with GelCode Blue (Pierce Chemical, Rockford, IL); the <50-kDa band obtained in the GST-CD2AP 3.SH3 domain pulldown was excised from the gel and in-gel-digested with trypsin. Peptides were loaded onto a reverse-phase microcapillary high-performance liquid chromatography column (Vydac, Grace, Deerfield, IL) and eluted into a Finnigan LCQ ion-trap mass spectrometer (Thermo Scientific, West Palm Beach, FL) with a linear gradient of 100% RP-A buffer (0.1% formic acid, 5% acetonitrile) to 40% RP-A plus 60% RP-B buffer (0.1% formic acid, 80% acetonitrile). The tandem mass spectrometry spectra were searched against the human, mouse, and rat protein databases (www.ncbi.nlm.nih.gov) using the SEQUEST program (Eng *et al.*, 1994), and the results were filtered and sorted using DTASelect (Tabb *et al.*, 2002). Immunoblotting was performed as in Lehtonen *et al.* (2004, 2008a), and blots were quantified using an Odyssey Infrared Imaging System (LI-COR, Lincoln, NE).

Antibodies

Rabbit anti–CD2AP 209, 211, and 1774 were raised against aa 331–637 (Lehtonen *et al.*, 2008b), aa 1–330 (Lehtonen *et al.*, 2008b), and aa 6–574 (Lehtonen *et al.*, 2000) of mouse CD2AP. Rabbit anti–CD2AP (H290) and anti–septin 7 (H120) and goat anti–septin 7 (N12) were from Santa Cruz Biotechnology (Santa Cruz, CA). Rabbit septin 7 (C) was from Immuno-Biological Laboratories (Gumma, Japan). An additional rabbit anti–septin 7 was kindly provided by Christine Field (Harvard Medical School, Boston, MA) and anti–septin 9 and anti–septin 11 were kindly provided by Koh-ichi Nagata (Aichi Human Service Center, Japan). Rabbit antibody against nephrin (#1034) is described in Ahola *et al.* (2003). The other antibodies used were: mouse anti–Pan Akt (R&D Systems, Minneapolis, MN); rabbit anti–phospho-Akt (Ser-473) (Cell Signaling Technology, Danvers, MA); mouse anti-VAMP2 (Synaptic System, Goettingen, Germany); mouse anti-actin and rabbit anti–syntaxin 4 (Sigma-Aldrich).

Immunoperoxidase staining

Kidney samples were fixed with 10% Formalin, dehydrated, and embedded in paraffin. Immunoperoxidase staining was performed with a VectaStain Elite kit (Vector Laboratories, Burlingame, CA). Sections were deparaffinized, antigen retrieval was done by boiling for 15 min in a microwave oven in 10 mM citric acid (pH 6.0), and endogenous peroxidase was inactivated by incubation in 0.5% H_2O_2 in methanol for 30 min. Sections were blocked with CAS-block (Zymed, San Francisco, CA) and incubated with anti–septin 7 antibody diluted in ChemMate (DakoCytomation, Glostrup, Denmark) and with biotinylated goat anti-rabbit secondary antibody followed by incubation with ABC reagent and AEC (DakoCytomation) color development. Sections were counterstained with hematoxylin and mounted with Shandon Immu-Mount (Thermo Scientific, Waltham, MA).

Indirect immunofluorescence

Rat kidney cryosections were fixed with acetone, blocked with CAS-BLOCK (Invitrogen), and stained with affinity-purified anti–CD2AP 211 and anti–septin 7 (N12) diluted in ChemMate (DakoCytomation) at 4°C overnight, which was followed by detection with Alexa Fluor 555 donkey anti-rabbit and Alexa Fluor 488 donkey anti-goat IgGs (Molecular Probe, Eugene, OR). Human podocytes were treated with 5 μM cytochalasin D (Sigma-Aldrich) for 30 min. Mouse podocytes were serum-starved for 20 h and stimulated with 20 nM insulin (NovoNordisk, Bagsværd, Denmark) for 15 min. HIRc cells were transfected with siRNAs as described in *Silencing septin 7 by siRNA*, serum-starved for 16 h, and stimulated with 200 nM insulin (NovoNordisk) for 15 min. Cells were fixed with 2% paraformaldehyde for 30 min; blocked in 2% FCS, 2% bovine serum albumin, and 0.2% fish skin gelatin; and incubated with primary antibodies at room temperature for 1 h. Detection was with Alexa Fluor 555 donkey anti-mouse and Alexa Fluor 488 donkey anti–rabbit IgGs (Molecular Probes). Actin stress fibers were visualized with rhodamine phalloidin (Molecular Probes), and nuclei were

visualized with Hoechst 33342 (Sigma-Aldrich). Samples were examined with a Zeiss Axioplan2 microscope (Thornwood, NY).

Immunoprecipitation

Lysates were precleared with protein A-Sepharose (Invitrogen) or TrueBlot anti–rabbit or anti–mouse Ig IP beads (eBiosciences, San Diego, CA) and incubated with CD2AP 209, CD2AP 211, septin 7 (H120), or VAMP2 antibodies and normal rabbit serum or rabbit/mouse IgG (Zymed) as controls at 4°C for 16 h. The immune complexes were bound to protein A-Sepharose or TrueBlot beads, washed with lysis buffer, and immunoblotted.

Silencing septin 7 by siRNA

Human podocytes and HIRc cells were transfected with 100 nmol ON-TARGET plus SMARTpool human Sept7 (L-011607-00-0005), rat Sept7 (L-093922-01-0010), or siCONTROL Non-Targeting Pool#2 (D-001206-14-05) siRNA (Dharmacon, Lafayette, CO) using Lipofectamine 2000 (Invitrogen). Cells were used for experiments after 48 h at 33°C (podocytes) or 72 h at 37°C (HIRc).

2-Deoxy-D-glucose uptake assay

HIRc cells transfected with septin 7 siRNA were serum-starved for 16 h and treated or not with 200 nM insulin for 15 min in Krebs Ringer phosphate buffer (128 mM NaCl, 1.4 mM $CaCl_2$, 1.4 mM MgSO4, 5.2 mM KCl, 10 mM Na_2HPO_4, pH 7.4). Alternatively, starved HIRc cells were treated with 50 μM FCF (Sigma-Aldrich) or dimethyl sulfoxide (DMSO) for 4 h at 33°C and stimulated with insulin as above. Mouse podocytes were serum-starved for 20 h, incubated with 50 μM FCF as above, and treated or not with 20 nM insulin for 15 min. Cells were exposed to 50 μmol/l (1 μCi/ml) 2-deoxy-D-[(1, 2-^{3}H(N)]-glucose (Perkin Elmer-Cetus, Boston, MA) for 5 min at 37°C (HIRc) or 33°C (podocytes), washed with ice-cold PBS, and solubilized in 1% Triton X-100 in PBS. β-Emission was measured by Wallac 1450 MicroBeta TriLux Liquid Scintillation Counter (Perkin Elmer-Cetus).

Retroviral infection

HEK293FT cells were cotransfected with pKAT2 and full-length rat nephrin cDNA in pLNCX2 (Lehtonen *et al.*, 2004) or pLNCX2 alone using Lipofectamine 2000. Medium containing the virus was used to infect HIRc cells (as in Lehtonen *et al.*, 2004) transfected 16 h earlier with septin 7 siRNA. Cells were lysed 48 h after infection.

Statistical analysis

Results are presented as mean ± SD. Statistical analysis was performed using Student's *t* test (Microsoft Excel, Redmond, WA).

ACKNOWLEDGMENTS

We thank Moin Saleem (Academic Renal Unit, Southmead Hospital, Bristol, UK) for kindly providing conditionally immortalized human podocyte cell line AB 8/13, Jerrold Olefsky (University of California, San Diego, La Jolla, CA) for HIRc cells, Koh-ichi Nagata (Aichi Human Service Center, Japan) for septin 7 fusion protein constructs and septin 9 and septin 11 antibodies, Harry Holthöfer (Dublin City University, Ireland) for anti-nephrin antibody, and Christine Field (Harvard Medical School, Boston, MA) for anti-septin 7 antibody. Fang Zhao is acknowledged for his help with confocal microscopy, and Anna-Reetta Salonen and Niina Ruoho are thanked for technical help. This work was supported by the Academy of Finland (121248, 131255, 218021; S.L.), the European Research Council (242820; S.L.), the Helsinki Biomedical Graduate Program (A.W.) and National Institutes of Health (NIH) P41 RR011823 (J.R.Y.).

REFERENCES

Ahola H, Heikkila E, Astrom E, Inagaki M, Izawa I, Pavenstadt H, Kerjaschki D, Holthofer H (2003). A novel protein, densin, expressed by glomerular podocytes. J Am Soc Nephrol 14, 1731–1737.

Beites CL, Campbell KA, Trimble WS (2005). The septin Sept5/CDCrel-1 competes with α-SNAP for binding to the SNARE complex. Biochem J 385, 347–353.

Beites CL, Xie H, Bowser R, Trimble WS (1999). The septin CDCrel-1 binds syntaxin and inhibits exocytosis. Nat Neurosci 2, 434–439.

Cormont M, Meton I, Mari M, Monzo P, Keslair F, Gaskin C, McGraw TE, Le Marchand-Brustel Y (2003). CD2AP/CMS regulates endosome morphology and traffic to the degradative pathway through its interaction with Rab4 and c-Cbl. Traffic 4, 97–112.

Coward RJ, Welsh GI, Koziell A, Hussain S, Lennon R, Ni L, Tavare JM, Mathieson PW, Saleem MA (2007). Nephrin is critical for the action of insulin on human glomerular podocytes. Diabetes 56, 1127–1135.

Coward RJ *et al.* (2005). The human glomerular podocyte is a novel target for insulin action. Diabetes 54, 3095–3102.

Dustin ML *et al.* (1998). A novel adaptor protein orchestrates receptor patterning and cytoskeletal polarity in T-cell contacts. Cell 94, 667–677.

Eng JK, McCormack AL, Yates JR, III (1994). An approach to correlate tandem mass spectral data of peptides with amino acid sequences in a protein database. J Am Soc Mass Spectrom 5, 976–89.

Haarer BK, Pringle JR (1987). Immunofluorescence localization of the *Saccharomyces cerevisiae* CDC12 gene product to the vicinity of the 10-nm filaments in the mother-bud neck. Mol Cell Biol 7, 3678–3687.

Hall PA, Jung K, Hillan KJ, Russell SE (2005). Expression profiling the human septin gene family. J Pathol 206, 269–278.

Hall PA, Russell SE (2004). The pathobiology of the septin gene family. J Pathol 204, 489–505.

Hartwell LH (1971). Genetic control of the cell division cycle in yeast. IV: Genes controlling bud emergence and cytokinesis. Exp Cell Res 69, 265–276.

Hsu SC, Hazuka CD, Roth R, Foletti DL, Heuser J, Scheller RH (1998). Subunit composition, protein interactions, and structures of the mammalian brain sec6/8 complex and septin filaments. Neuron 20, 1111–1122.

Hu Q, Nelson WJ, Spiliotis ET (2008). Forchlorfenuron alters mammalian septin assembly, organization, and dynamics. J Biol Chem 283, 29563–29571.

Iwase M, Okada S, Oguchi T, Toh-e A (2004). Forchlorfenuron, a phenylurea cytokine, disturbs septin organization in *Saccharomyces cerevisiae*. Genes Genet Syst 79, 199–206.

Joberty G, Perlungher RR, Sheffield PJ, Kinoshita M, Noda M, Haystead T, Macara IG (2001). Borg proteins control septin organization and are negatively regulated by Cdc42. Nat Cell Biol 3, 861–866.

Kestila M *et al.* (1998). Positionally cloned gene for a novel glomerular protein–nephrin–is mutated in congenital nephrotic syndrome. Mol Cell 1, 575–582.

Kim HB, Haarer BK, Pringle JR (1991). Cellular morphogenesis in the *Saccharomyces cerevisiae* cell cycle: localization of the CDC3 gene product and the timing of events at the budding site. J Cell Biol 112, 535–544.

Kinoshita M (2003). The septins. Genome Biol 4, 236.

Kinoshita M, Field CM, Coughlin ML, Straight AF, Mitchison TJ (2002). Self- and actin-templated assembly of mammalian septins. Dev Cell 3, 791–802.

Kinoshita M, Kumar S, Mizoguchi A, Ide C, Kinoshita A, Haraguchi T, Hiraoka Y, Noda M (1997). Nedd5, a mammalian septin, is a novel cytoskeletal component interacting with actin-based structures. Genes Dev 11, 1535–1547.

Kirsch KH, Georgescu MM, Shishido T, Langdon WY, Birge RB, Hanafusa H (2001). The adapter type protein CMS/CD2AP binds to the proto-oncogenic protein c-Cbl through a tyrosine phosphorylation-regulated Src homology 3 domain interaction. J Biol Chem 276, 4957–4963.

Kremer BE, Adang LA, Macara IG (2007). Septins regulate actin organization and cell-cycle arrest through nuclear accumulation of NCK mediated by SOCS7. Cell 130, 837–850.

Lehtonen S, Lehtonen E, Kudlicka K, Holthofer H, Farquhar MG (2004). Nephrin forms a complex with adherens junction proteins and CASK in podocytes and in Madin-Darby canine kidney cells expressing nephrin. Am J Pathol 165, 923–936.

Lehtonen S, Ora A, Olkkonen VM, Geng L, Zerial M, Somlo S, Lehtonen E (2000). In vivo interaction of the adapter protein CD2-associated protein with the type 2 polycystic kidney disease protein, polycystin-2. J Biol Chem 275, 32888–32893.

Lehtonen S, Shah M, Nielsen R, Iino N, Ryan JJ, Zhou H, Farquhar MG (2008a). The endocytic adaptor protein ARH associates with motor and centrosomal proteins and is involved in centrosome assembly and cytokinesis. Mol Biol Cell 19, 2949–2961.

Lehtonen S, Tienari J, Londesborough A, Pirvola U, Ora A, Reima I, Lehtonen E (2008b). CD2-associated protein is widely expressed and differentially regulated during embryonic development. Differentiation 76, 506–517.

Lehtonen S, Zhao F, Lehtonen E (2002). CD2-associated protein directly interacts with the actin cytoskeleton. Am J Physiol Renal Physiol 283, F734–F43.

Monzo P, Gauthier NC, Keslair F, Loubat A, Field CM, Le Marchand-Brustel Y, Cormont M (2005). Clues to CD2-associated protein involvement in cytokinesis. Mol Biol Cell 16, 2891–2902.

Nagata K, Asano T, Nozawa Y, Inagaki M (2004). Biochemical and cell biological analyses of a mammalian septin complex, Sept7/9b/11. J Biol Chem 279, 55895–55904.

Oegema K, Savoian MS, Mitchison TJ, Field CM (2000). Functional analysis of a human homologue of the *Drosophila* actin binding protein anillin suggests a role in cytokinesis. J Cell Biol 150, 539–552.

Orlando RA, Takeda T, Zak B, Schmieder S, Benoit VM, McQuistan T, Furthmayr H, Farquhar MG (2001). The glomerular epithelial cell anti-adhesin podocalyxin associates with the actin cytoskeleton through interactions with ezrin. J Am Soc Nephrol 12, 1589–1598.

Palmen T, Lehtonen S, Ora A, Kerjaschki D, Antignac C, Lehtonen E, Holthofer H (2002). Interaction of endogenous nephrin and CD2-associated protein in mouse epithelial M-1 cell line. J Am Soc Nephrol 13, 1766–1772.

Rothman JE (1994). Intracellular membrane fusion. Adv Second Messenger Phosphoprotein Res 29, 81–96.

Saleem MA, O'Hare MJ, Reiser J, Coward RJ, Inward CD, Farren T, Xing CY, Ni L, Mathieson PW, Mundel P (2002). A conditionally immortalized human podocyte cell line demonstrating nephrin and podocin expression. J Am Soc Nephrol 13, 630–638.

Schiffer M, Mundel P, Shaw AS, Bottinger EP (2004). A novel role for the adaptor molecule CD2-associated protein in transforming growth factor-β-induced apoptosis. J Biol Chem 279, 37004–37012.

Schmidt K, Nichols BJ (2004). Functional interdependence between septin and actin cytoskeleton. BMC Cell Biol 5, 43.

Shankland SJ (2006). The podocyte's response to injury: role in proteinuria and glomerulosclerosis. Kidney Int 69, 2131–2147.

Shih NY, Li J, Cotran R, Mundel P, Miner JH, Shaw AS (2001). CD2AP localizes to the slit diaphragm and binds to nephrin via a novel C-terminal domain. Am J Pathol 159, 2303–2308.

Shih NY, Li J, Karpitskii V, Nguyen A, Dustin ML, Kanagawa O, Miner JH, Shaw AS (1999). Congenital nephrotic syndrome in mice lacking CD2-associated protein. Science 286, 312–315.

Söllner T, Whiteheart SW, Brunner M, Erdjument-Bromage H, Geromanos S, Tempst P, Rothman JE (1993). SNAP receptors implicated in vesicle targeting and fusion. Nature 362, 318–324.

Tabb DL, McDonald WH, Yates JR, III (2002). DTASelect and Contrast: tools for assembling and comparing protein identifications from shotgun proteomics. J Proteome Res 1, 21–26.

Tejada T, Catanuto P, Ijaz A, Santos JV, Xia X, Sanchez P, Sanabria N, Lenz O, Elliot SJ, Fornoni A (2008). Failure to phosphorylate AKT in podocytes from mice with early diabetic nephropathy promotes cell death. Kidney Int 73, 1385–1393.

Vega IE, Hsu SC (2003). The septin protein Nedd5 associates with both the exocyst complex and microtubules and disruption of its GTPase activity promotes aberrant neurite sprouting in PC12 cells. Neuroreport 14, 31–37.

Weber T, Zemelman BV, McNew JA, Westermann B, Gmachl M, Parlati F, Sollner TH, Rothman JE (1998). SNAREpins: minimal machinery for membrane fusion. Cell 92, 759–772.

Welsch T, Endlich N, Kriz W, Endlich K (2001). CD2AP and p130Cas localize to different F-actin structures in podocytes. Am J Physiol Renal Physiol 281, F769–F77.

Welsh GI *et al*. (2010). Insulin signaling to the glomerular podocyte is critical for normal kidney function. Cell Metab 12, 329–340.

Yaddanapudi S *et al*. (2011). CD2AP in mouse and human podocytes controls a proteolytic program that regulates cytoskeletal structure and cellular survival. J Clin Invest. 121, 3965–3980.